

PREPARED FOR SUBMISSION TO JINST

23<sup>RD</sup> INTERNATIONAL WORKSHOP ON RADIATION IMAGING DETECTORS

26–30 JUNE 2022

RIVA DEL GARDA, ITALY

## Characterisation of Gamma-irradiated MCz-Silicon Detectors with a High- $K$ Negative Oxide as Field Insulator

---

S. Bharthuar,<sup>a,b,1</sup> M. Bezak,<sup>a,c</sup> E. Brücken,<sup>a,b</sup> A Gädda,<sup>f</sup> M. Golovleva,<sup>a,c</sup> A. Karadzhinova-Ferrer,<sup>a,c,e</sup> A. Karjalainen,<sup>c</sup> N. Kramarenko,<sup>a,c</sup> S. Kirschenmann,<sup>a,b</sup> P. Luukka,<sup>a,c</sup> J. Ott,<sup>d</sup> E. Tuominen,<sup>a,b</sup> M. Väänänen.<sup>a,c</sup>

<sup>a</sup>Helsinki Institute of Physics, Gustaf Hällströmin katu 2, FI-00014, Finland

<sup>b</sup>Department of Physics, University of Helsinki, Gustaf Hällströmin katu 2, FI-00014, Finland

<sup>c</sup>Lappeenranta-Lahti University of Technology, Yliopistonkatu 34, Lappeenranta, FI-53850, Finland

<sup>d</sup>SCIPP, University of California Santa Cruz, CA 95064, USA

<sup>e</sup>Ludong University, Yantai, China

<sup>f</sup>Okmetic Oy., Piitie 2, Vantaa, FI-01510, Finland

E-mail: [shudhashil.bharthuar@cern.ch](mailto:shudhashil.bharthuar@cern.ch)

**ABSTRACT:** The high-luminosity operation of the Tracker in the Compact Muon Solenoid (CMS) detector at the Large Hadron Collider (LHC) experiment calls for the development of silicon-based sensors. This involves implementation of AC-coupling to micro-scale pixel sensor areas to provide enhanced isolation of radiation-induced leakage currents. The motivation of this study is the development of AC-pixel sensors with negative oxides (such as aluminium oxide - Al<sub>2</sub>O<sub>3</sub> and hafnium oxide - HfO<sub>2</sub>) as field insulators that possess good dielectric strength and provide radiation hardness. Thin films of Al<sub>2</sub>O<sub>3</sub> and HfO<sub>2</sub> grown by atomic layer deposition (ALD) method were used as dielectrics for capacitive coupling. A comparison study based on dielectric material used in MOS capacitors indicate HfO<sub>2</sub> as a better candidate since it provides higher sensitivity (where, the term sensitivity is defined as the ratio of the change in flat-band voltage to dose) to negative charge accumulation with gamma irradiation.

Further, space charge sign inversion was observed for sensors processed on high resistivity p-type Magnetic Czochralski silicon (MCz-Si) substrates that were irradiated with gamma rays up to a dose of 1 MGy. The inter-pixel resistance values of heavily gamma irradiated AC-coupled pixel sensors suggest that high- $K$  negative oxides as field insulators provide a good electrical isolation between the pixels.

**KEYWORDS:** Radiation-hard detectors, Solid state detectors, Particle tracking detectors, Si pad detectors

ARXIV EPRINT: [1234.56789](https://arxiv.org/abs/1234.56789)

---

<sup>1</sup>Corresponding author.

---

## Contents

|          |   |          |
|----------|---|----------|
| <b>1</b> | <b>Introduction</b>   | <b>1</b> |
| <b>2</b> | <b>Samples Measured and Methods</b>   | <b>2</b> |
| <b>3</b> | <b>Characterisation of Gamma Irradiated MOS Capacitors with high-<math>K</math> negative oxides</b>     | <b>3</b> |
| <b>4</b> | <b>Radiation Hardness Studies of Gamma Irradiated Detectors</b>   | <b>4</b> |
| 4.1      | I-V/C-V measurements of Gamma-irradiated PIN Diode Structures   | 4        |
| 4.2      | Transient Current Technique (TCT) measurements  | 5        |
| 4.3      | Inter-pixel resistance measurements for non-irradiated and gamma-irradiated AC coupled pixel detectors. | 7        |
| <b>5</b> | <b>Conclusion and Discussions</b>   | <b>8</b> |

---

## 1 Introduction

Silicon-based particle detectors are implemented in the Large Hadron Collider (LHC) experiment for vertex and track reconstruction of charged particles. However, with the upgrade of the LHC to High-luminosity LHC (HL-LHC), pixel detectors, in particular those located close to the interaction point, will be subjected to a radiation-hard environment. This leads to a degradation of their electrical properties due to radiation-induced damage [1]. For instance, in the HL-LHC operation of the CMS Tracker detector, the innermost silicon layers will be exposed to radiation levels increasing up to a magnitude of  $> 2 \times 10^{16} n_{eq} \text{cm}^{-2}$ , and 12 MGy [2].

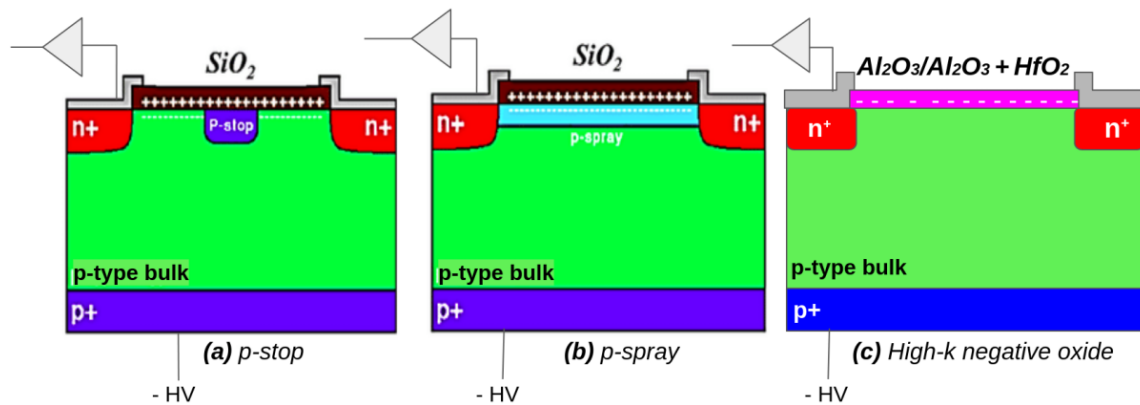


**Figure 1.** Schematic representation showing electrical isolation between two adjacent pixels in a DC-coupled pixel detector where (a) p-stop, (b) p-spray or (c) a high- $K$  negative oxide material like  $\text{Al}_2\text{O}_3$  or  $\text{Al}_2\text{O}_3 + \text{HfO}_2$  is used as an inter-pixel isolation strategy.

These high doses of radiation levels deteriorate the performance of the silicon detectors. This includes an decrease in their signal-to-noise ratio due to an increase in the leakage current as well as a reduction in the charge collection efficiency due to radiation induced defects. Thus, in order to alleviate these challenges, unlike the traditionally used DC-coupled (conductively-coupled) detectors that are susceptible to an increased level in leakage current values, AC-coupled (capacitively-coupled) pixel detectors are anticipated to be operational as particle tracking devices in future collider experiments. Conventionally, as shown in Figures 1a and 1b, the pixels are electrically isolated from each other by the use of p-stop or p-spray in order to avoid the creation of a short-circuiting channel between the pixelated n<sup>+</sup>-implants that could be generated due to the accumulation of electrons under the silicon-dioxide (positive oxide) dielectric layer. However, introduction of p-stop and p-spray requires additional implantation processing steps, which subject the silicon wafers to high temperatures and increases the mask levels that reduce the cost-effectiveness of the finally processed detectors. Alternatively as a solution, shown in Figure 1c, the segmented implants can be electrically isolated from each other by utilising Atomic Layer Deposition (ALD)-grown thin films of negative oxides with a high *K*-value (Al<sub>2</sub>O<sub>3</sub> and HfO<sub>2</sub>) as insulating layers that possess high negative oxide charge concentration values of the order of magnitude of 10<sup>11</sup>–10<sup>13</sup> cm<sup>-2</sup>. This corroborates higher oxide capacitance values for an improved capacitive coupling [3]. ALD ensures in providing high uniformity thin films of Al<sub>2</sub>O<sub>3</sub> and HfO<sub>2</sub> with good accuracy, deposited at comparatively low temperatures (typically ~300°C). This prevents the wafers from being subjected to additional mask levels and high temperature implantation processes.

## 2 Samples Measured and Methods

All the samples were fabricated on p-type (boron-doped) Magnetic Czochralski (MCz) 6” silicon wafers from Okmetic Oy. The silicon wafers possess a resistivity and thickness of ~4-8 kΩ-cm and 320 μm, respectively. Fabrication of the devices measured in this study have been provided in articles [4–6].

The following study focuses on investigating the robustness and the impact of mostly gamma irradiation, up to a dose of 1 MGy, on ALD-grown Al<sub>2</sub>O<sub>3</sub> or HfO<sub>2</sub> + Al<sub>2</sub>O<sub>3</sub> implemented as a field insulator in Metal-Oxide-Semiconductor (MOS) capacitors (with a gate of 1.5 mm in diameter), as well as in capacitive coupling for n<sup>+</sup>/p<sup>-</sup>/p<sup>+</sup> prototypes of PIN diode (where the active area of the pad is 7.2 × 7.2 mm<sup>2</sup>) and AC-coupled pixel detectors (similar to the PSI46dig design consisting of 52 × 80 pixel matrix, along with a pitch size of 150 × 100 μm) [13]. Previous studies in [7] show that an additional layer of HfO<sub>2</sub> along with Al<sub>2</sub>O<sub>3</sub> incorporated in MOS devices provides a higher capacitive coupling along with a better insulation, reduced susceptibility to an early breakdown, higher sensitivity to proton irradiation specifically at high fluences, and an improved radiation hardness. Additionally, electrical characterisation studies were performed on the non-irradiated and gamma-irradiated sensors to study the electric field within the bulk of PIN diode prototypes and inter-pixel resistance in AC-coupled pixel sensors.

### 3 Characterisation of Gamma Irradiated MOS Capacitors with high- $K$ negative oxides

Capacitance-versus-Voltage measurements (C-V) of MOS capacitors can be used to determine the effective fixed oxide and mobile charges of the insulating layer by extracting the flat-band voltage ( $V_{fb}$ ).  $V_{fb}$  is defined as the gate voltage value at which the the energy band of the silicon substrate is flat at the oxide-substrate interface. In ideal conditions,  $V_{fb}$  is of a magnitude of -0.54 V for MOS devices with aluminum as the metal gate and a silicon substrate with a doping concentration of  $8 \times 10^{11} \text{ cm}^{-3}$ . The shift in the flat-band voltage ( $\Delta V_{fb}$ ) value from its ideal condition gives an estimation of effective fixed oxide charge density value ( $N_f$ ) in the dielectric layer that are incorporated during the thin films growth or deposition processes. Figure 2a shows the C-V curves

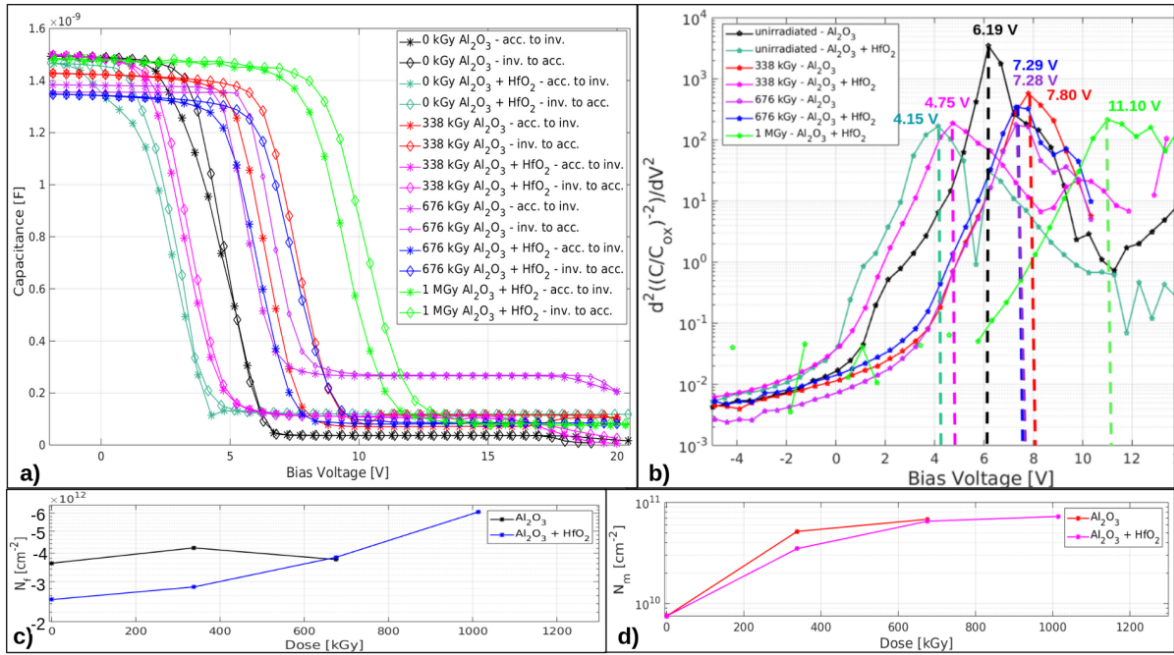


**Figure 2.** **a)** C-V curves for non-irradiated and gamma-irradiated MOS capacitors with  $\text{Al}_2\text{O}_3$  and  $\text{Al}_2\text{O}_3 + \text{HfO}_2$  as the dielectric layer, measured by scanning the bias voltage from accumulation to inversion mode of operation and vice-versa at a constant frequency of 1 kHz. **b)** Estimation of  $V_{fb}$  from C-V curves, where the bias voltage is scanned from accumulation to inversion region, as the peak bias voltage value, extracted by double-differentiating  $C/C_{ox}$  curve with respect to bias voltage. Variation in concentration of effective **c)** fixed oxide charges ( $N_f$ ) and **d)** mobile oxide charges ( $N_m$ ) with gamma dose.

for MOS capacitors with either  $\text{Al}_2\text{O}_3$  or  $\text{Al}_2\text{O}_3 + \text{HfO}_2$  as the oxide layer irradiated with gamma-rays at doses of 338 kGy, 676 kGy and 1 MGy. The capacitance values were recorded with an LCR meter at a frequency of 1 kHz and an AC signal amplitude of 998.5 mV. The bias voltage was swept from accumulation to inversion operation mode and vice-versa in order to determine the hysteresis of the C-V curve. The hysteresis in the C-V curves is a measure of another non-ideal condition in MOS capacitors, associated to origin of the mobile charge density ( $N_m$ ), due to the trapping of charges induced in the oxide layer in the fabrication steps and contamination during the irradiation campaigns [8, 9]. As shown in Figure 2b,  $V_{fb}$  for samples scanned from accumulation to inversion

conditions, is extracted from C-V curves by differentiating the  $(C/C_{\text{ox}})^{-2}$  versus bias voltage curve twice. The gate voltage value corresponding to the peak in the double differentiated curve is equal to the  $V_{\text{fb}}$  value. Usually, second differentiation introduces a great deal of noise as the bias voltage sweeps toward the deep-depletion region but that can be avoided by smoothing the data [10].  $N_f$  is determined using the following relation:

$$N_f = \frac{\Delta V_{\text{fb}} \times C_{\text{ox}}}{eA} \quad (3.1)$$

where,  $e$  is the fundamental unit of charge,  $A$  refers to the cross-sectional area of the gate and  $C_{\text{ox}}$  is the capacitance value estimated from the accumulation region of the C-V plots. In a similar manner effective concentration of mobile charge density ( $N_m$ ) can be determined using the following relation:

$$N_m = -\frac{\Delta V_{\text{hysteresis}} \times C_{\text{ox}}}{eA} \quad (3.2)$$

where  $\Delta V_{\text{hysteresis}}$  is the hysteresis in the flat-band voltage attained while sweeping the gate voltage from accumulation to inversion region and vice-versa. It is evident in Figure 2c that the effective concentration of fixed oxide charges increases by a factor of  $\sim 2.44$  on irradiation up to doses of 1 MGy for samples with an additional dielectric layer of  $\text{HfO}_2$  along with  $\text{Al}_2\text{O}_3$ . As the concentration of the negative charge accumulated in the oxide-silicon substrate interface increases with gamma irradiation, it leads to energy band bending further down in equilibrium. Therefore, in order to attain flat-band condition, the gate bias has to be swept towards higher positive bias voltage values in order to overcome the inherent bending of the bands. Figure 2d shows that  $N_m$  values increase with gamma dose. MOS samples with  $\text{Al}_2\text{O}_3 + \text{HfO}_2$  show higher sensitivity towards gamma irradiation up to a dose of 676 kGy as the effective  $N_m$  values increases by a factor of  $\sim 2.3$  more than that for samples with  $\text{Al}_2\text{O}_3$  alone as dielectric layer. Further, on irradiating the MOS samples up to 1 MGy, devices with  $\text{Al}_2\text{O}_3$  alone as field insulator layer were susceptible to an early breakdown.

## 4 Radiation Hardness Studies of Gamma Irradiated Detectors

### 4.1 I-V/C-V measurements of Gamma-irradiated PIN Diode Structures

Figure 3a shows current-versus-voltage (I-V) curves of non-irradiated and gamma-irradiated PIN diode prototype with  $\text{Al}_2\text{O}_3$  as the dielectric material that were measured at  $-20^\circ\text{C}$ . The leakage current shown in the figure corresponds to the values read out from the active pad region consisting of the pn-junction. The first guard ring surrounding the pad was grounded. The non-irradiated samples possess low leakage currents of a magnitude of a few  $\sim 100$  pA. However, the edge effects of the sensors contribute to a high total current, thereby terminating the measurements as the current value reached its compliance of  $50 \mu\text{A}$ . Interestingly, the compliance is not attained for gamma-irradiated sensors. The gamma-irradiated sensors could be biased up to a voltage of  $\sim 900$  V before the total current reaches a compliance value of 1 mA. The pad current values for sensors irradiated up to doses of 338 kGy and 676 kGy is increased by a factor of approximately 1.25 and 3, respectively; while the pad current value for the sensor irradiated at 1 MGy is increased by  $\sim 2$  orders of magnitude. Figure 3b shows inverse-squared capacitance versus bias voltage plots derived

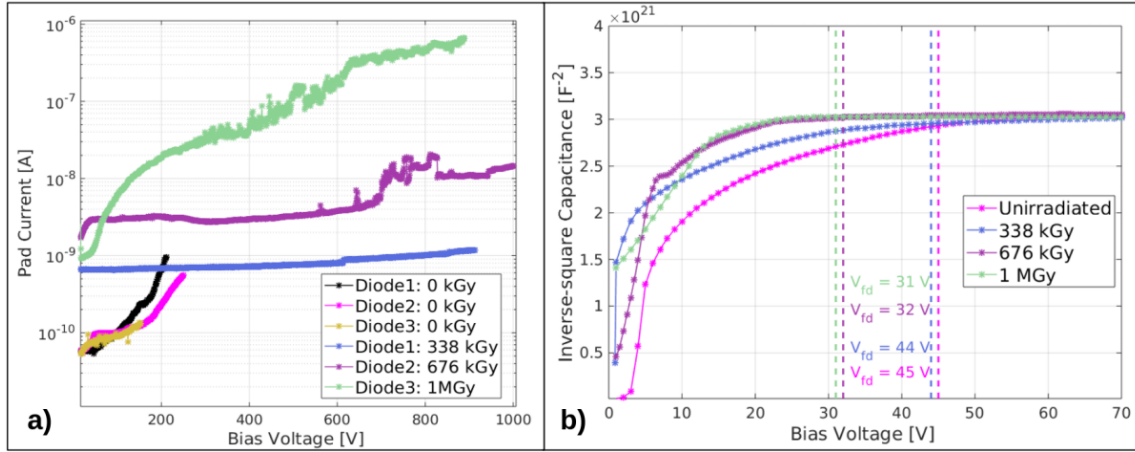


**Figure 3.** a) I-V and b) C-V measurements of non-irradiated and gamma-irradiated PIN diodes with Al<sub>2</sub>O<sub>3</sub> as field insulator. C-V measurements were performed at a frequency of 10 kHz.

from C-V measurements performed at a frequency of 10 kHz on the non-irradiated and gamma-irradiated PIN diodes. The full depletion voltage ( $V_{fd}$ ) of the non-irradiated sensors is  $\sim 50$  V. The  $V_{fd}$  value does not vary on irradiating the sensor up to 338 kGy. However,  $V_{fd}$  value is reduced by  $\sim 20$  V on irradiating up to doses of 676 kGy and 1 MGy. This corresponds to an effective doping concentration value of  $6.69 \times 10^{11} \text{ cm}^{-3}$  for non-irradiated sensor that subsequently gets reduced by a factor of 1.71 on irradiating it at 1 MGy.

## 4.2 Transient Current Technique (TCT) measurements

Single Photon Absorption (SPA)-TCT is an electrical characterisation method that makes use of a fast pulse infrared (IR) laser imitating a minimum ionising particle (MIP). The photons of the IR laser traverse through the active region of the detector thereby leading to a continuous energy deposition along the beam direction that provides a close approximation to high-energy particles interacting with the detector and the signal read-out is due to the charge carriers that are generated within the bulk of the depleted region. According to the Shockley-Ramo theorem [11], the resulting transient signal detected by the oscilloscope provides information about the movement of the charge carriers due to the electric field within the sensor. The collected charge across the depleted bulk can be investigated by integrating the induced current signal over time as the IR laser beam is scanned across the depth of the detector. This methodology of projecting the laser beam across the edge of the sensor to study the charge collection and drift velocity profiles is called edge-TCT (e-TCT). Moreover, the electric field inside a PIN diode can be studied from the drift velocity, which itself can be extracted from the waveform using the prompt current method [12].

The full depletion voltage for the non-irradiated device, based on the charge collection profiles, was estimated to be approximately close to 95 V using e-TCT with SPA, as shown in Figure 4a. The attained  $V_{fd}$  value analysed in e-TCT measurements was  $\sim 45$  V higher than the value extracted from the C-V measurements for non-irradiated and irradiated sensors. The reason behind this feature was the high voltage filter connected to the bias line that supplies a lower bias value to the device under test compared to the actual applied voltage from the Keithley, due to the high total leakage

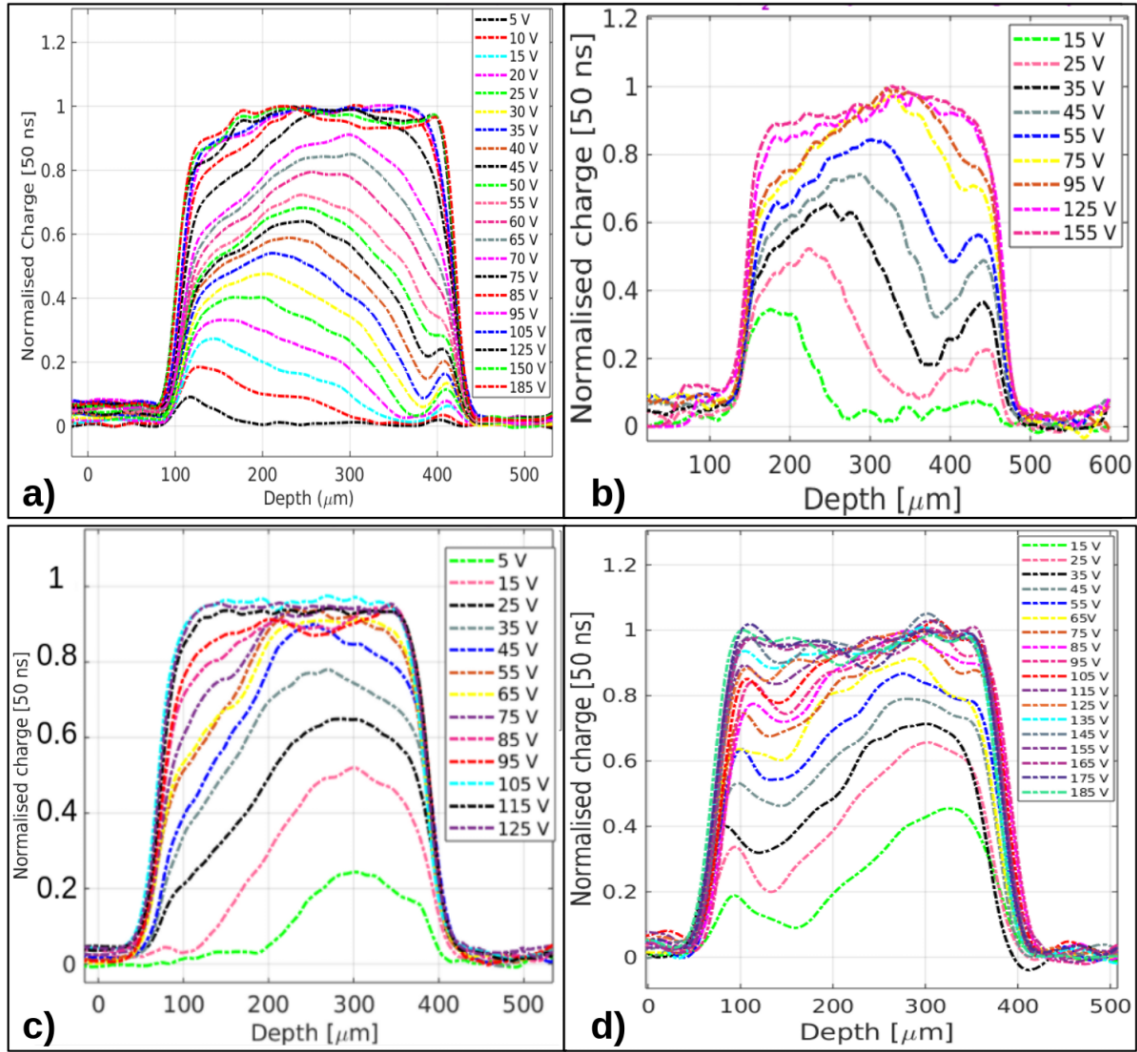


**Figure 4.** Charge collection versus depth profiles at varying bias voltages of **a)** non-irradiated and gamma-irradiated sensors at doses of **b)** 338 kGy, **c)** 676 kGy and **c)** 1 MGy measured using e-TCT. The left and right-hand sides of the profiles refer to the front and rear sides of the sensor, respectively. All the irradiated sensors were measured at a temperature of  $-20^{\circ}\text{C}$ .

current read out from the sensors.

Further, the charge collection profiles as shown in Figures 4b, 4c and 4d show that the full depletion voltage value is reduced by  $\sim 20$  V, when irradiating the samples up to 1 MGy. The charge collection profiles are coherent to the drift velocity profiles of irradiated sensors, shown in Figure 5c and 5d, that demonstrate space charge sign inversion of the bulk as the depletion initiates from the back-plane. This feature gets more prominent on samples irradiated at a dose of 1 MGy in comparison to the ones irradiated at 676 kGy. No significant change in the drift velocity profiles were observed in a non-irradiated sensor and a detector irradiated up to an accumulated dose of 338 kGy, as analysed in Figure 5a and 5b. This suggests that the depletion in unirradiated devices and in samples irradiated up to a dose value of 338 kGy occurs starting from the  $n^+$ -implants located

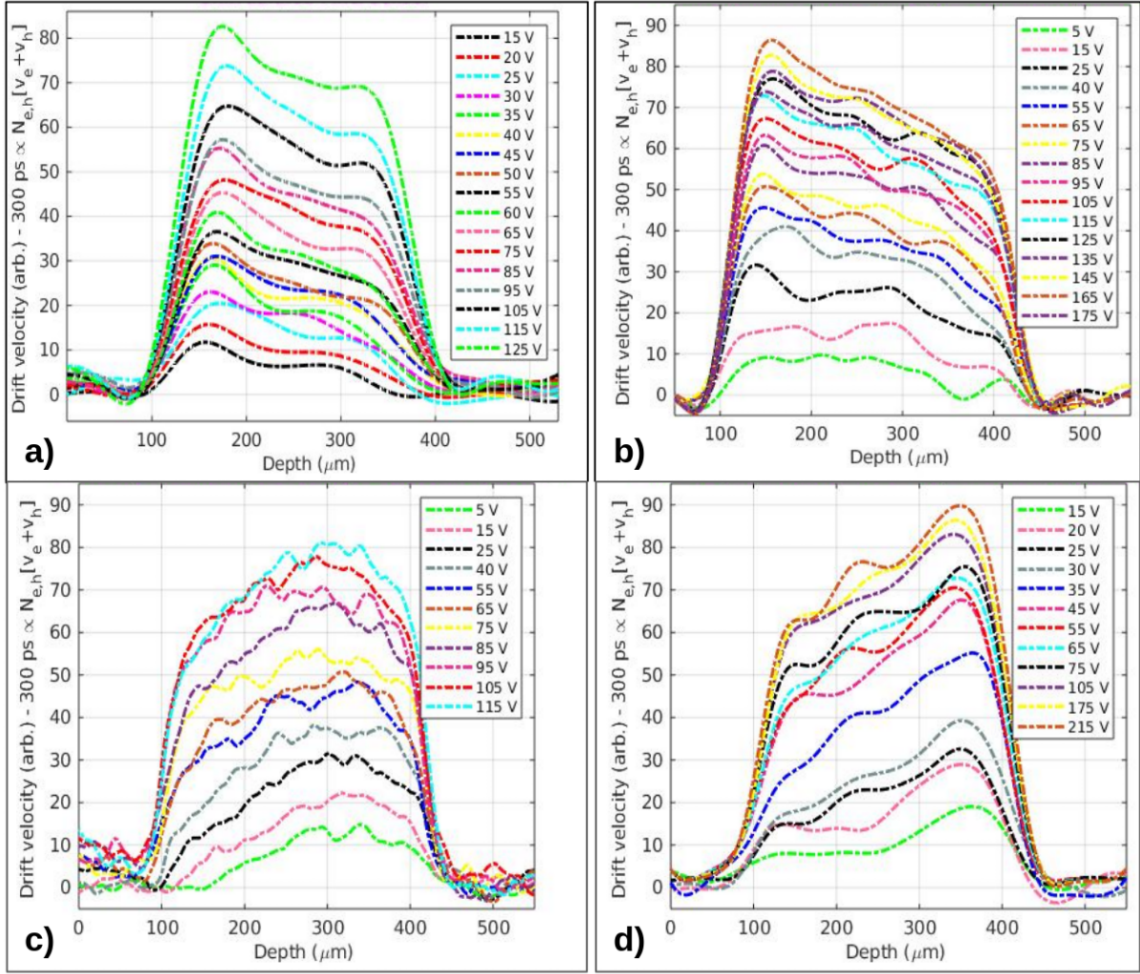


**Figure 5.** Drift velocity versus depth profiles at varying bias voltages for sensors **a)** non-irradiated and irradiated with gamma-rays up to dose values of **b)** 338 kGy, **c)** 676 kGy and **d)** 1 MGy measured using e-TCT. The left and right-hand sides of the profiles refer to the front and rear sides of the sensor, respectively. All the irradiated sensors were measured at a temperature of  $-20^{\circ}\text{C}$ .

at the top of the sensors.

### 4.3 Inter-pixel resistance measurements for non-irradiated and gamma-irradiated AC coupled pixel detectors.

Inter-pixel resistance was measured at bias voltage values from 180–220 V for non-irradiated and gamma-irradiated AC-coupled pixel sensors. During the measurements, the current was read out from the DC-pad of an arbitrary pixel in the centre of a  $3 \times 3$  matrix while the adjacent pixels surrounding it were grounded. The inter-pixel resistance value of non-irradiated devices was of a magnitude  $\sim 10 \text{ M}\Omega$ , equivalent to DC-coupled pixel sensors with same pitch size [14, 15]. As shown in Figure 6, the magnitude of inter-pixel resistance value was reduced by a factor of 6 on irradiating the sensors to a dose of 1 MGy as the leakage current increases by  $\sim 2$  orders of magnitude due to radiation induced damage. The lower limit of the inter-pixel resistance is given by



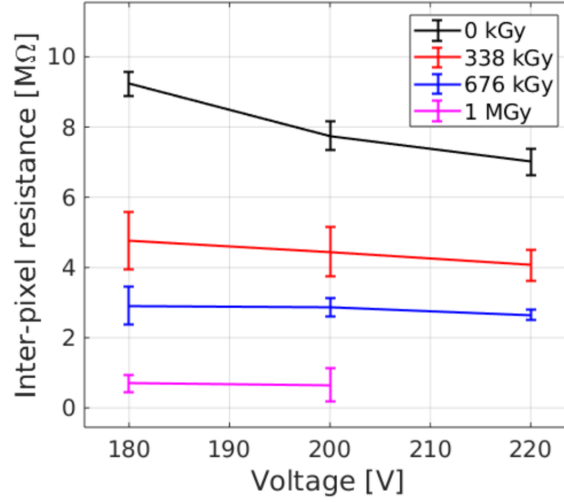


**Figure 6.** Variation of inter-pixel resistance values measured for AC-coupled pixel detectors irradiated with Co-60 gamma ray source up to dose of 1 MGy.

the requirement of preventing a significant signal distribution to the neighboring channels within a typical shaping time of 25 ns. This leads to a lower limit of the resistance of about 1 MΩ in case of p-stop and p-spray implemented as pixel isolation strategies. The measured inter-pixel resistance values for detectors with Al<sub>2</sub>O<sub>3</sub> as field insulator, irradiated up to a dose of 1 MGy, lie within this minimum requirement.

## 5 Conclusion and Discussions

Characterization of MOS devices with high-*K* negative oxide indicates that a negative charge accumulation is induced by gamma irradiation based on the study of the flat-band voltage. The negative oxide charge during the irradiation is an essential prerequisite of radiation hardness resiliency of n<sup>+</sup>/p<sup>-</sup>/p<sup>+</sup> (n-on-p) particle detectors widely intended to be used in future high-luminosity experiments. MOS devices with Al<sub>2</sub>O<sub>3</sub> + HfO<sub>2</sub> possess higher sensitivity to gamma irradiation in comparison to samples with Al<sub>2</sub>O<sub>3</sub> alone as an insulating layer.

A reduction in full-depletion voltage value and space charge sign inversion was observed in sensors irradiated with gamma rays up to a dose of 1 MGy. Additional investigation is ongoing using Deep-Level Transient Spectroscopy (DLTS) and Thermally Stimulated Current (TSC) methods to understand the defects introduced in the sensors that could possibly explain the reason for space charge sign inversion observed in e-TCT measurements. However, the inter-pixel resistance values show promising results for both non-irradiated and gamma irradiated AC-coupled pixel sensors with high-*K* negative oxide as field insulator as the pixels are electrically isolated from each other, even for heavily irradiated devices.

## Acknowledgments

S. Bharthuar would like to acknowledge the Magnus Ehrnrooth Foundation for financial support. Facilities for detector fabrication were provided by Micronova Nanofabrication Centre in Espoo,

Finland. The samples were irradiated with Co-60 gamma ray source at the Laboratory for Radiation Chemistry and Dosimetry (LRKD), in Ruđer Bošković Institute, Croatia. The C-V, I-V, and e-TCT measurements were performed at the Detector Laboratory in Helsinki Institute of Physics.

## References

- [1] M. Moll, *Displacement Damage in Silicon Detectors for High Energy Physics*, (*IEEE Trans Nucl Sci* **65** (2018) 1561-1582).
- [2] S. Orfanelli for CMS collaboration, *The Phase 2 Upgrade of the CMS Inner Tracker*, (*NIM-A* **980** (2020) 164396).
- [3] J. Härkönen et al., *Processing of  $n^+/p^-/p^+$  strip detectors with atomic layer deposition (ALD) grown  $Al_2O_3$  field insulator on magnetic Czochralski silicon (MCz-Si) substrates*, *NIM-A* **828** (2016) 46-51.
- [4] J. Ott et al., *Processing of AC-Coupled N-In-P Pixel Detectors on MCz Silicon Using Atomic Layer Deposited Aluminium Oxide.*, *NIM-A* **958** (2020) 162547.
- [5] A. Gädda et al., *AC-coupled N-In-P Pixel Detectors on MCz Silicon with Atomic Layer Deposition (ALD) Grown Thin Film.*, *NIM-A* **986** (2021) 164714.
- [6] J. Ott et al., *Characterization of Magnetic Czochralski Silicon Devices with Aluminium Oxide Field Insulator: Effect of Oxygen Precursor on Electrical Properties and Radiation Hardness.*, *J. Inst.* **16** (2021) P05011.
- [7] S. Bharthuar et al., *Characterization of Heavily Irradiated Dielectrics for Pixel Sensors Coupling Insulator Applications*, *Front. Mater.* **8** (2022) 769947.
- [8] F.M.Fowkes et al., *Electric fields at the surface and interface of  $SiO_2$  films on silicon*, *Surf. Sci* **13** (1969) 184-195.
- [9] J. L. Repace et al., *Radiation-Induced Increase of Mobile Sodium in MOS Capacitors*, *IEEE Trans Nucl Sci* **24** (1977) 2088-2092.
- [10] D. K. Schroder, *Semiconductor Material Device Characterization*, Wiley Interscience, New York (1998).
- [11] S. Ramo, *Currents Induced by Electron Motion*, *J. Appl. Phys.* **27** (1939) 584-585.
- [12] C. Canali et al., *Electron and hole drift velocity measurements in silicon and their empirical relation to electric field and temperature*, *IEEE Trans Electron Devices* **22** (1975) 1045-1047.
- [13] Gray, J. A., *The CMS Phase-1 pixel detector*, *J. Inst.* **8** (2013) C12047.
- [14] V. Bonvicini et al., *Simulating capacitive cross-talk effects in DC-coupled hybrid silicon pixel detectors*, *NIM-A* **372** (1996) 793-110.
- [15] M.S Alam, *The ATLAS silicon pixel sensors*, *NIM-A* **456** (2001) 217-232.